Submitted to ADVANCED ENERGY MATERIALS

DOI: 10.1002/aenm.1400334
Article first published online: 22 APR 2014

Metallic Photonic Crystal Absorber-Emitter for Efficient Spectral Control in High-Temperature Solar Thermophotovoltaics

Veronika Rinnerbauer, Andrej Lenert, David M. Bierman, Yi Xiang Yeng, Walker R. Chan, Robert D. Geil, Jay J. Senkevich, John D. Joannopoulos, Evelyn N. Wang, Marin Soljačić, and Ivan Celanovic*

V. Rinnerbauer, Y. X. Yeng, W. R. Chan, J. J. Senkevich, Prof. J. D. Joannopoulos, Prof. M. Soljačić, Ivan Celanovic
Research Laboratory of Electronics, Massachusetts Institute of Technology,
77 Massachusetts Avenue, MA, Cambridge 02139, USA
E-mail: veronika.rinnerbauer@jku.at
A. Lenert, D. M. Bierman, Prof. E. N. Wang
Department of Mechanical Engineering, Massachusetts Institute of Technology,
Cambridge, MA 02139 USA
R. D. Geil
Department of Applied Physical Sciences, University of North Carolina,
223 Chapman Hall, Chapel Hill 27599, USA

Keywords: metallic photonic crystals, selective absorbers, selective emitters, solar energy conversion, solar thermophotovoltaics

A high-temperature stable solar absorber based on a metallic 2D photonic crystal (PhC) with high and tunable spectral selectivity is demonstrated and optimized for a range of system conditions of operating temperature and irradiance. In particular a PhC absorber with solar absorptance $\bar{\alpha} = 0.86$ and thermal emittance $\bar{\varepsilon} = 0.26$ at 1000 K, using high-temperature material properties, is achieved resulting in a thermal transfer efficiency more than 50 % higher than that of a blackbody absorber. Furthermore, an integrated double-sided 2D PhC absorber/emitter pair is demonstrated for a high-performance solar thermophotovoltaic (STPV) system. The 2D PhC absorber/emitter is fabricated on a double-side polished tantalum substrate, characterized, and tested in an experimental STPV setup along with a flat Ta absorber and a nearly-blackbody absorber composed of an array of multi-walled carbon nanotubes (MWNTs). At an irradiance of 130 kWm^{-2} the PhC absorber enables more than a two-fold improvement in measured STPV system efficiency (3.74 %) relative to the nearly-blackbody absorber (1.60 %) and higher efficiencies are expected with increasing operating

temperature. These experimental results show unprecedented high efficiency, demonstrating the importance of the high selectivity of the 2D PhC absorber and emitter for high-temperature energy conversion.

1. Introduction

A high-performance selective absorber is a critical component in energy conversion systems such as solar thermal, solar thermochemical, and solar thermophotovoltaics. There exist a range of solutions with high absorptivity for low and intermediate temperatures.[1-3] However, for many applications, high operating temperatures (>700 K) are advantageous to achieve higher system efficiencies. Conventional absorbers are unsuitable at these high operating temperatures since there are more considerations to be taken into account.[4] Firstly, the materials and structures need to be thermally stable and maintain their optical properties at these high temperatures. Refractory metals are most advantageous due to their high melting point and low vapor pressure. Secondly, it is crucial that the absorber exhibits spectrally selective absorptance; namely high absorptivity in the shorter wavelength range to absorb most of the solar spectrum and low absorptivity (i.e., emissivity) in the longer wavelength range to minimize losses due to re-emission. Furthermore, this selectivity, i.e., the spectral range of high and low absorptivity, has to be tailored for the specific system operating conditions to achieve maximum system efficiency.

It is therefore advantageous to use PhCs which offer the possibility to tailor the spectral absorptance[5,6] and thus optimize system efficiency. Several absorbers based on 1D multilayer stacks,[7,8] 2.5D structures like pyramids,[9-11] 3D PhCs in refractory metals,[12,13] as well as metamaterials[14-16] have been proposed. In this work, we demonstrate the suitability of a 2D PhC comprising a square lattice of cylindrical cavities etched into a Ta substrate as a highly efficient and selective absorber at high temperatures, i.e., above 1000 K. While all of the above approaches achieve good spectral selectivity, the 2D PhC design is a compact and

thermally robust structure, minimizing the number of interfaces as compared to multilayer or 3D PhC approaches which is crucial for high temperature stability. At the same time,fabrication is simple and scalable and can be achieved by standard semiconductor processes. In this 2D PhC design, the absorptivity of the material is selectively enhanced by the introduction of cavity modes and the range of enhancement, i.e., high absorptivity, can be tuned by the geometric parameters of the cavities while keeping the emittance at long wavelengths low. A thin HfO_2 coating is introduced to serve both as a surface protection coating to enhance stability at high temperature[17-20] as well as an efficient antireflection (AR) coating maximizing absorptance in the visible and near infrared.

In this paper, the performance of the PhC absorber is optimized in section 2 and compared to that of both unstructured flat Ta and a nearly-blackbody absorber for a range of system conditions of operating temperature and irradiance. In section 3, the specific case of a solar thermophotovoltaic (STPV) system is studied, where operating temperature and irradiance are interdependent. Both the PhC absorber and PhC emitter are optimized to achieve a maximum STPV system efficiency at a realistic target operating temperature of 1300 K. Finally in section 4, a selective PhC absorber/emitter pair is presented in an experimental STPV setup.

The experimental realization of a STPV system with highly spectral selective surfaces for both absorber and emitter in a compact planar design presented in this study achieves unprecedented high system efficiency as compared to previous systems using non-selective surfaces.[21,22] In the STPV system, an intermediate stage of a combined absorber and emitter between the incident solar radiation and the photovoltaic (PV) cell serves as a conversion step to convert the broadband solar spectral radiation to thermal spectral radiation that is ideally narrow-band and spectrally matched to the bandgap of the PV cell (**Figure 1**).[23-25] For this energy conversion stage, an integrated selective absorber/emitter pair in a planar configuration is proposed where both the absorber and the emitter side are based on the 2D PhC however with different geometrical parameters. This selective PhC absorber/emitter is

fabricated on a double-side polished polycrystalline Ta substrate and studied experimentally in an STPV setup. The system efficiency is measured and the performance of the selective PhC absorber is compared to that of a flat Ta absorber and of a nearly-blackbody absorber composed of an array of multi-walled carbon nanotubes (MWNTs), all with the same PhC emitter side and using the same experimental setup. The experimental results match the predictions from the detailed system modeling. An unprecedented high system efficiency of 3.74 % at 130 suns (130 kWm^{-2}) is achieved which is 2.3 times that measured for the blackbody absorber and 2.8 times that expected for a blackbody absorber/emitter pair, demonstrating the superior performance of the selective PhC absorber/emitter design in this configuration.

2. Selective Absorbers

The key metrics for solar absorbers are the solar absorptivity $\bar{\alpha}$ defined as the fraction of solar irradiation absorbed (we use AM1.5 direct plus circumsolar throughout) and the thermal emissivity $\bar{\varepsilon}$ defined as the ratio of energy emitted by the absorber compared to the blackbody at the operating temperature T: [26]

$$\bar{\alpha} = \frac{1}{H_S}\int_0^\infty d\lambda \varepsilon(\lambda) S_S(\lambda) \quad (1)$$

$$\bar{\varepsilon} = \frac{\int_0^\infty d\lambda \varepsilon(\lambda)/\{\lambda^5(e^{\frac{hc}{\lambda kT}}-1)\}}{\int_0^\infty d\lambda/\{\lambda^5(e^{\frac{hc}{\lambda kT}}-1)\}} \quad (2)$$

where $S_s(\lambda)$ is the solar spectrum (AM1.5D), H_S is the total solar irradiance of this spectrum, $\varepsilon(\lambda)$ is the spectral emittance of the absorber, λ is the wavelength of light, T is the operating temperature, h is the Planck constant, c is the speed of light, and k is the Boltzmann constant. Since there is an angular dependence of the spectral emittance for most absorbers, the hemispherically integrated emittance is used in Equation 2 to calculate the thermal emissivity $\bar{\varepsilon}$. To determine the solar absorptivity $\bar{\alpha}$, the normal spectral emissivity is used for radiation incident at normal angle. Alternatively, the dependence of the averaged absorptivity on the

opening angle of the incident radiation is calculated using the angular dependent emissivity integrated over the solid angle up to the opening angle in Equation 1.

For common solar absorbers used in solar thermal applications at intermediate temperatures (up to 700 K), it is relatively easy to achieve both high solar absorptivity and low thermal emissivity at the same time, since blackbody emission in the near IR is low at those temperatures and the thermal and solar spectra do not overlap significantly. However, there is a trade-off between the two parameters; at higher temperatures a sharp cut-off between high absorptance and low emittance regions is crucial. In Figure 1(b) this trade-off is graphically depicted via the overlap of the incident irradiation spectrum (AM1.5D) and the emission spectrum of a blackbody at 1300 K as an example. Considering Kirchhoff's law which states that for a body in thermal equilibrium, the absorptivity is equal to the emissivity at every wavelength, i.e., $\alpha(\lambda,T)=\varepsilon(\lambda,T)$, we cannot simultaneously achieve high absorptivity and low emissivity in the overlapping wavelength range. The ideal absorber is therefore given by a step function (see Figure 1(b)) with an absorptivity of 1 in the visible and zero absorptivity in the infrared, with a cut-off wavelength between the two that depends on the operating temperature and the power density or concentration of the incident radiation.[7] We can define the thermal transfer efficiency η_T of the absorber as the difference between input and output power normalized by the incident power: [8]

$$\eta_T = \overline{\alpha} - \overline{\varepsilon} \cdot \frac{\sigma T^4}{H_s} \qquad (3)$$

with the solar absorptivity $\overline{\alpha}$ and the thermal emissivity $\bar{\varepsilon}$ as defined above and σ being the Stefan-Boltzmann constant. Since real absorber materials have an absorptance spectrum that may deviate considerably from the ideal step function – in particular, the emittance at long wavelengths being above zero – the thermal transfer efficiency is a more useful figure of merit when comparing and optimizing absorber materials than using the cut-off wavelength

alone. Essentially, it corresponds to the fraction of power incident on the absorber which is available for useful energy conversion.

We optimize the PhC absorber on a Ta substrate using this figure of merit for different operating conditions, starting with the benchmark of 1000 K, 100 suns (i.e., 100 kWm^{-2}).[8] To calculate the PhC spectral emittance, we use both the Finite-Difference-Time-Domain method (FDTD, incorporated via Meep)[27] as well as the Fourier Modal Method (incorporated via S^4)[28]. The PhC layout is a square array of cylindrical cavities with radius *r*, period *a,* and depth *d* etched into the Ta substrate. The material dispersion of Ta and its dependence on the temperature is taken into account using a Drude-Lorentz model. It is essential to correctly simulate the optical properties of the PhC at high operating temperatures, as the emissivity of most materials increases with increasing temperature, and, as a consequence, the emissivity of the PhC fabricated from this substrate material also depends on temperature.[17] To calculate the optical properties of the PhC at high temperature the model is therefore fit to the optical properties of Ta taken from literature for high temperature.[29] For simulations at room temperature, which we use to compare with reflectance measurements taken at room temperature, the reflectance of polished substrates measured at room temperature is used to fit the Drude-Lorentz model. The optimization of the PhC parameters is performed using nonlinear global optimization algorithms (incorporated via NLopt)[30] where the absorptivity at normal incidence and the emissivity averaged over hemispherical emission are taken into account.

The spectral absorptance at normal incidence and the hemispherically averaged spectral emittance of the PhC optimized for 1000 K and 100 suns are shown in in Figure 1(c). The optimized PhC has a radius r=0.34 µm, period a=0.78 µm, and depth d=8.0 µm (**Table 1**). As can be seen, the PhC allows for a selective increase of the absorptivity in the short wavelength range, while keeping the emissivity low at longer wavelengths. The range of high absorptivity is given by the cavity modes introduced by the PhC and can be varied by tuning the

geometrical parameters of the PhC.[31] In addition to the high spectral selectivity that can be achieved by this PhC design, there is an angular dependence of the spectral emittance of the PhC, which further enhances the selectivity of the PhC absorber. This is because the hemispherically averaged spectral emittance for the PhC is lower than the spectral absorptance, as long as the irradiation is not incident from all directions (or mainly at large incident angles). Ideally the aperture angle of the concentrating or optical system used to irradiate the absorber is less than 60° and centered near normal incidence.

In **Figure 2,** the calculated thermal transfer efficiency of the Ta PhC absorber as a function of operating temperature and incident (normal) irradiance is compared to that of a blackbody absorber and of unstructured flat Ta. Note that the geometrical parameters and simulated spectra of the PhC absorbers optimized for different operating conditions differ. As can be seen, the blackbody absorber has a better performance (η_T) than the selective PhC absorber for low temperature and high irradiance (reaching more than 0.8 for <1200 K and >300 suns), since for these conditions the emission is low and the absorptivity of the absorber has more significant impact on η_T than its emissivity. However, the maximum temperature that can be reached with blackbody absorbers for a given irradiance is very limited due to high losses by re-emission. For an irradiance of 100 suns, the maximum temperature with a positive thermal transfer efficiency using the blackbody absorber is about 1150 K, which would limit the efficiency of an energy conversion system like STPV. To facilitate high operating temperature at moderate to low irradiance, it is imperative to use selective absorbers. With the PhC absorber, even at 100 suns an operating temperature above 1400 K can be reached. For the PhC absorber, a solar absorptivity of 0.81 and a thermal emissivity of 0.256 is achieved at 1000 K resulting in a thermal transfer efficiency of 66.4% for an irradiance of 100 suns. In contrast, the thermal transfer efficiency of a blackbody absorber for these conditions is only 43.3% (see Table 1). The emissivity values of the Ta PhC are higher than some previously reported for selective absorbers, with calculated solar absorptivity of around 0.9 and thermal

emissivity as low as 0.15 using cones or multilayer structures based on Mo and W.[7,8,32] The higher emissivity calculated here, and consequently lower absorptivity of the optimized PhC, is due to the fact that high-temperature material data is used for Ta to simulate the optical properties of the PhC at high temperature, as discussed above. In fact, the lower limit of the thermal emissivity for the PhC absorber is that of the flat substrate, which is 0.139 at 1000 K for Ta and 0.17 for W and increases with temperature. Unstructured flat Ta also has some intrinsic selectivity (see Figure 1(c)). Therefore it is likewise possible to reach a high operating temperature with a flat Ta absorber (1400 K at 100 suns) but never with good efficiency (only 30 % for 100 suns, 1000 K) due to the lower absorptivity (see Table 1).

3. Selective Absorbers for Solar Thermophotovoltaics

In a solar thermophotovoltaic system, the operating parameters of temperature and irradiance are not independent. The irradiance needed to reach a certain operating temperature is set by the power balance of input and output power, including all losses. Using this power balance, the thermal transfer efficiency of the absorber in the STPV system can be rewritten as:

$$P_{total} = \overline{\alpha} \cdot H_s = (\overline{\varepsilon}_{absorber} + \overline{\varepsilon}_{emitter} + \overline{\varepsilon}_{side} \cdot f) \cdot \sigma T^4 = \overline{\varepsilon}_{total} \cdot \sigma T^4 \quad (4)$$

$$\eta_T = \overline{\alpha}\left(1 - \frac{\overline{\varepsilon}_{absorber}}{\overline{\varepsilon}_{total}}\right) \quad (5)$$

$$H_s = \frac{\overline{\varepsilon}_{total} \cdot \sigma T^4}{\overline{\alpha}} \quad (6)$$

where $\overline{\alpha}$ is the solar absorptivity as defined in Equation 1 and $\bar{\varepsilon}_{absorber}$, $\bar{\varepsilon}_{emitter}$, and $\bar{\varepsilon}_{side}$ are the thermal emissivity of the absorber, emitter, and side surfaces respectively at a certain temperature as defined in Equation 2, and f is the area ratio of side surface to absorber (or emitter, both having the same area).

In this approximation, losses are restricted to the radiative losses from all surfaces, including absorber, emitter, and side losses, and isothermal operation of the absorber/emitter pair is assumed where T=T(absorber)=T(emitter). The parameters of the absorber are optimized with

Equation 5 for maximum thermal transfer efficiency η_T at a certain target temperature using the thermal emissivity of all surfaces at this temperature, and the irradiance needed to reach this temperature is calculated using Equation 6. For this optimization, the hemispherically averaged thermal emissivity of a PhC emitter $\overline{\varepsilon}_{emitter}$ is used and optimized for an InGaAsSb PV cell with a bandgap at 2.3 µm. The thermal emissivity of the sides $\overline{\varepsilon}_{side}$ is calculated for flat Ta and the area ratio of side surface to absorber (or emitter) *f* is assumed to be 0.2 (as for a 1 cm² sample with a thickness of 0.5 mm).

The normal absorptance spectrum of the PhC absorber optimized for a target operating temperature of 1300 K is shown in **Figure 3**. The optimized parameters of this PhC absorber are a radius r=0.28 µm, period a=0.66 µm, and depth d=4.6 µm (Table 1). As can be seen, the absorptivity is high from the visible to the near IR with a steep drop for wavelengths above approximately 1 µm. The absorptivity in the visible, however, is limited by diffraction, which occurs on the PhC lattice for wavelengths below the period of the PhC (at normal incidence). There is for this reason an unfortunate dip of the absorptivity around 500 nm, corresponding exactly to the peak of the solar spectrum, which is also shown for comparison in Figure 3(a). One approach to relieve this limitation is to use an antireflection coating for this wavelength range in addition to the PhC structure. To this end, a thin coating of HfO_2 was used, which has shown excellent stability at high temperature and serves as a thermal barrier coating and surface protection for the Ta PhC.[17]

Several studies have shown that microstructured surfaces experience a high risk of structural degradation at the high operating temperatures and long operational lifetimes expected in a TPV system.[17,33,34] The main effects driving thermal degradation are surface diffusion, surface reactions with oxygen and carbon in particular, and material stress. Grain growth and recrystallization play an additional role in the case of polycrystalline materials. It is essential to protect the PhC surface from these effects, and it has been shown that a conformal surface

coating of 20 nm HfO_2 ensures the thermal stability of both the structure and its optical properties in long-term tests at temperatures up to 1300 K.[17,18, 35]

To maximize the benefit of this coating as an antireflection coating in the visible, the thickness of the HfO_2 layer was optimized. Since the coating is deposited conformally by atomic layer deposition (ALD) on the PhC, the radius of the PhC cavities needs to be adapted taking into account this layer of higher refractive index on the cavity walls. As the optical path length in the cavity is effectively increased by the higher refractive index material on the sidewalls, the cut-off wavelength shifts to longer wavelengths for constant cavity radius. The thickness and radius of the PhC with the HfO_2 coating are again optimized for the maximum thermal transfer efficiency in the STPV system. The calculated efficiency as well as the optimized parameters of the PhC absorber for the STPV condition are listed in Table 1. With the coating, the solar absorptivity can be increased by 6.7 % (absolute) from 79.7 % to 86.4 % and the thermal transfer efficiency by 4.6 % from 47.1 % to 51.7 % as compared to the uncoated PhC absorber at normal incidence.

As discussed, the absorptivity is a function of incident angle, which is an advantage as long as the irradiating light is not incident from all directions. Of course the angle of incidence depends on the optics of the system used to achieve the necessary concentration. Figure 3(b) shows the dependence of the solar absorptivity on the opening angle of the incident irradiation, defined as half the aperture angle of the concentration optics (from the surface normal, see inset). As can be seen, the absorptivity remains high with a negligible decrease of absorptivity up to an opening angle of 30°; only for completely hemispherical incidence (opening angle of 90°) does the absorptivity drop sharply. Therefore, two limiting cases for the STPV system (independently from the concentration needed) are discussed in this study: first, irradiation with light at normal incidence, i.e., the aperture angle or numerical aperture is zero; and second, irradiation with light incident equally from all directions, i.e., a hypothetical aperture

angle of 180° or numerical aperture going to 1. The latter worst case limit is referred to as 'wide-angle incidence' in the following discussion.

4. Solar Thermophotovoltaic System with Selective PhC Absorber and Emitter

A solar thermophotovoltaic (STPV) system is demonstrated using a selective Ta PhC absorber and emitter fabricated on two sides of the same substrate, with the selective emitter matched to an InGaAsSb PV cell with a bandgap at approximately 2.3 μm (0.54 eV).[36] The selective PhC emitter has the same basic design as the absorber, but its parameters were optimized for maximum spectral efficiency η_{sp} at the target operating temperature of 1300 K. The spectral efficiency η_{sp} is defined as the ratio of (useful) thermal emission below the target bandgap at 2.3 μm to the total thermal emission at a certain target temperature [8] and is used as a figure of merit for the optimization, which is more robust than simply aligning the cut-off wavelength of the emitter with the bandgap of the PV cell:

$$\eta_{sp} = \frac{\int_0^{\lambda_{PV}} d\lambda\varepsilon(\lambda)/\{\lambda^5(\mathrm{e}^{\frac{hc}{\lambda kT}}-1)\}}{\int_0^{\infty} d\lambda\varepsilon(\lambda)/\{\lambda^5(\mathrm{e}^{\frac{hc}{\lambda kT}}-1)\}} \quad (7)$$

where λ_{PV} is the wavelength corresponding to the bandgap of the PV cell, i.e., the upper limit of the external quantum efficiency and therefore the useful wavelength range of the PV cell.

The selective PhC absorber is optimized as discussed above for maximum thermal transfer efficiency in the considered STPV system at a target operating temperature of 1300 K. The geometric parameters and spectral efficiency of the optimized PhC emitter are listed in Table 1 along with those of the optimized PhC absorber. The performance of the Ta PhC absorber in the STPV system is compared to the flat polished Ta absorber, and to a nearly-blackbody MWNT array absorber,[22,37] all with the same Ta PhC emitter and an absorber/emitter area ratio of 1. The realization of the selective absorber and emitter on the two sides of the same substrate has the advantage of facilitating direct thermal contact with minimal losses due to heat transport between the two. In addition the planar design is very thin and compact

reducing thermal radiation losses from the sides, and promoting structural stability at high operating temperatures.

The optical properties of the fabricated absorbers and emitters are experimentally determined using reflectance measurements at room temperature via an integrating sphere accessory. Since the samples are opaque, the spectral emittance *E* can be determined from the measured reflectance *R* using $E(\lambda)=A(\lambda)=1-R(\lambda)$. The normal spectral emittance at room temperature obtained from these measurements is shown in **Figure 4** for the Ta PhC emitter, absorber, and flat Ta, all coated with HfO_2. The measured spectra agree very well with the simulated ones at room temperature, which gives us confidence to use the simulated emittance spectra, both for normal and hemispherical incidence, at high temperature (using material dispersion of Ta at high temperature in the simulation) for TPV system modeling.

The experimental STPV setup uses a Xe arc source with a filter to simulate the AM1.5D spectrum, while the irradiance incident on the absorber/emitter sample and thereby the temperature of the absorber/emitter pair is controlled from room temperature to about 1300 K. The experimental layout minimizes parasitic heat losses while allowing for precise alignment and gap control between the absorber-emitter and the PV cell, both mounted in a vacuum setup.[22] The photocurrent generated by the PV cell and the current-voltage (I-V) curves are measured at steady state operation as a function of the irradiance incident on the absorber. The STPV system efficiency is calculated as the ratio of the measured electrical output power at the maximum power point of the PV cell to the input power.

The STPV system efficiency determined from the experiment is shown in **Figure 5** with a clear improvement with increasing spectral selectivity from the nearly-blackbody absorber to the coated flat Ta absorber to the PhC absorber. Predictions using a detailed numerical model closely match the results. In the system model, we assume isothermal operation of the absorber/emitter pair, i.e., absorber and emitter being at the same operation temperature. The irradiance from the emitter incident on the PV cell is calculated from the emitter spectrum in

dependence of the operating temperature. The geometry, i.e., the finite size of the emitter and PV cell and the gap between them, resulting in cavity losses, is included via the viewfactor and the reflection from the PV cell is taken into account using the measured reflectance spectrum. The electrical output power of the PV cell generated at this irradiance on the PV cell is calculated for the maximum power point of the PV cell, using the PV parameters determined from the measured I-V curve.[38] To calculate the incident irradiance (on the absorber) needed to reach this operating temperature, we take into account the radiative losses from all surfaces (absorber, emitter, sides and support needles) as well as conduction losses through the supporting needles holding the absorber/emitter pair, and the solar absorptivity of the absorber. The system efficiency predicted by this model is given by the ratio of electrical output power to the incident power calculated at the same operating temperature. Using this model the system efficiency is calculated both for normal incidence as well as the wide-angle incidence limit, i.e. light incident equally from all directions as discussed above. Since the solar absorptivity of selective absorbers decreases with increasing incident angle, the system efficiency achieved in the wide-angle incidence limit is lower than for the limit of normal incidence. In the experimental setup, the opening angle of incidence depends on the concentration, and therefore experimental results are within those two boundaries (normal and wide-angle incidence) for the Ta PhC absorber as well as the flat Ta absorber.

The experimentally determined STPV system efficiency using the selective Ta PhC absorber is 3.74 ± 0.24 % achieving an electrical output power density of 0.49 Wcm^{-2} at an irradiance of 130 suns. This system efficiency is about 1.2 times higher than that of the coated flat Ta (3.16 ± 0.20 %) and 2.3 times higher compared to the nearly-blackbody absorber (1.60 ± 0.10 %) at a comparable irradiance of approximately 130 suns. Since all absorbers are coupled to the same PhC emitter and PV cell, this improvement is a direct consequence of the fact that the losses by the absorber are reduced and a higher operating temperature can be achieved with the selective PhC absorber at the same irradiance (about 1270 K compared to

1240 K and 1140 K for the flat Ta and nearly-blackbody absorber, respectively, at 130 suns) resulting in higher useful irradiance on the PV cell.

The measured efficiency with the 2D PhC absorber/emitter pair is also higher than previously reported for a 1D PhC emitter with an area-ratio optimized nearly-blackbody absorber of 3.2 ± 0.2 % at a similar operating temperature,[22] even with a non-optimized area ratio of the absorber and emitter. An STPV system efficiency of 0.8 % was reported at 1573 K in a previous study using a coated W absorber and emitter in an outdoor STPV experiment.[21] The improved system efficiency measured in this study is attributed to the high spectral selectivity of the 2D PhC absorber and emitter. As discussed, the selective PhC absorber achieves an improvement of 2.3 versus the blackbody absorber, using the same PhC emitter. To estimate the relative contribution of the selective PhC emitter to the system efficiency, we also calculate the expected system efficiency for a blackbody emitter in combination with the same absorbers, as shown in Figure 5(a). Since the spectral selectivity as defined in Equation 7 of a blackbody is only 8.6 % as compared to 47.1 % for the PhC emitter at 1300 K, the losses due to waste heat are much higher for the blackbody emitter. Therefore, the achievable STPV system efficiency is reduced, but also shifted to higher irradiance. For the blackbody absorber, the system efficiency is mostly dominated by the absorber losses due to re-emission. The improvement using a selective PhC emitter in comparison to the blackbody emitter is still high at low irradiance. At 130 suns, the blackbody absorber / blackbody emitter achieves only a system efficiency of 1.3 % as compared to the blackbody absorber / PhC emitter configuration reaching 1.6 %, which is an improvement of approximately a factor 1.2. For the selective PhC absorber, the improvement from the PhC emitter versus the blackbody emitter is even higher, resulting in a factor 1.8 improvement in the system efficiency between PhC absorber / blackbody emitter (2.1 %) and PhC absorber / PhC emitter (3.7 %) for the wide-angle incidence limit at 130 suns. Also, the maximum achievable system efficiency with the

PhC absorber/ blackbody emitter is limited to 4.5 % at normal incidence and an irradiance of 400 suns is needed to reach this operating point with a temperature of 1500 K.

The maximum system efficiency predicted by the model for the selective PhC absorber / PhC emitter pair is 5.46 % (absolute) at approximately 260 suns at normal incidence, and 4.65 % at 300 suns for the wide-angle incidence limit - both at an optimum operating temperature of about 1500 K, which was not measured due to experimental setup limitations. At higher temperatures, i.e., higher irradiance on the PV cell, the PV cell efficiency decreases rapidly, limited mostly by the series resistance of the PV cell.

To uncouple the efficiency of the absorber/emitter pair from the PV cell efficiency, we define the total optical conversion efficiency, η_{opt} as the ratio of useful irradiance reaching the PV cell, i.e., in the wavelength range with non-zero external quantum efficiency and including view factor and reflection on the PV cell, to the input power density, i.e., irradiance incident on the absorber.

$$\eta_{opt} = \frac{F_V}{H_S}\int_0^{\lambda_{PV}} d\lambda \varepsilon_{eff}(\lambda)\frac{2\pi hc^2}{\lambda^5(e^{\frac{hc}{\lambda kT}}-1)} \quad (8)$$

$$\eta_{STPV} = \eta_{opt} \cdot \eta_{PV} \quad (9)$$

where $\varepsilon_{eff}(\lambda)$ is the effective spectral emittance of the emitter, which is reduced due to the reflection from the absorber, and F_V is the viewfactor taking into account the separation of emitter and cell. This optical efficiency is as high as 18.8 % for the PhC absorber at normal incidence at 1300 K, compared to only 10.1 % for the blackbody absorber, and increasing with increasing temperature (see Figure 5(b)). In contrast, the efficiency of the PV cell is at its maximum of about η_{PV} = 24.8% at 1300 K, and it decreases with increasing emitter temperature, i.e., increasing irradiation.

A detailed analysis of the losses in the STPV system (Figure 5(c)) shows that even with the optimized selective PhC absorber at normal incidence at the target operating temperature of 1300 K as much as 43 % of the incident power is lost in the absorber, either by reflection

(8.5 %) or re-emission (34.5 %). In contrast, re-emission by the sides of the absorber/emitter pair, conductive losses through the supports (both less than 5 %), radiation by the support, and view factor losses (both less than 3 %) are minor contributions. Parasitic emission by the emitter (i.e., above bandgap) is the second largest contribution to the losses with 22.7 % of the input power. Therefore, improvements on the absorber side of the STPV system are critical and will have the highest impact on the overall system efficiency. One possibility to further reduce losses by re-emission of the absorber is to optimize the area ratio between the absorber and the emitter, which would allow to further increase selectivity of the absorber side.[22] Also, the use of a filter on the absorber side (reducing re-emission) could be advantageous as long as the transmission is not reduced. Furthermore, advances in the performance of the small bandgap PV cell, especially reducing the series resistance, have a direct impact on increasing the STPV system efficiency.

5. Conclusion

A selective solar absorber based on a 2D PhC made from Ta was studied for very high operating temperatures (above 1000 K). For this PhC absorber high spectral selectivity is achieved by cavity modes that selectively enhance the emissivity in a certain wavelength range, which can be tailored via the geometric parameters of the cavity. The thermal transfer efficiency of the absorber was used as a figure of merit to optimize the geometric parameters of the PhC for maximum performance. For an operating temperature above approximately 1000 K this selective PhC absorber has superior performance as compared to a blackbody absorber or the unstructured metal surface due to its high selectivity, which facilitates reaching high operating temperature with relatively low irradiance. For the PhC absorber, an averaged absorptivity of 0.81 and an emissivity of 0.256 was achieved at 1000 K, taking into account the high-temperature material properties of Ta. The resulting thermal transfer efficiency of the PhC absorber is 66.4 % for an irradiance of 100 suns, compared to 43.3 % for a blackbody absorber at the same conditions.

Furthermore, a selective 2D PhC absorber/emitter pair was demonstrated for the first time for a solar thermophotovoltaic application. In this planar configuration both sides of a flat Ta substrate were structured into a 2D PhC, which has the advantage of excellent thermal contact and low side losses. The PhC geometry of the emitter was optimized for maximum spectral efficiency at a target operating temperature of 1300 K, matched to an InGaAsSb PV cell with a bandgap at 2.3 μm. The absorber was optimized for thermal transfer efficiency at 1300 K, taking into account the power balance in the STPV system and radiation losses from all surfaces. In addition, a thin surface layer of HfO_2 was used as an antireflection coating in the visible for the absorber, while also increasing the thermal stability of the PhC. The proposed absorber/emitter pair was fabricated, its optical properties were characterized, and its performance was experimentally tested in an STPV setup together with an absorber based on flat Ta and a nearly-blackbody absorber composed of an array of MWNTs, all with the same PhC emitter side. The experimentally determined system performance agrees well with a detailed system model using the absorber and emitter spectral properties and taking into account all losses. The selective PhC absorber achieves a measured system efficiency of 3.74% at an irradiance of approximately 130 suns which is more than twice the performance of the nearly-blackbody absorber (1.60 %) at the same incident irradiance. It is also 17 % higher than previously reported for an area-ratio optimized nearly-blackbody absorber with a 1D PhC emitter (3.2 %) at a similar operating temperature,[22] which demonstrates the importance of high selectivity of the absorber and emitter for high-temperature energy conversion. The selective PhC emitter achieves an improvement in system efficiency of approximately a factor 1.8 compared to a blackbody emitter using the same PhC absorber at an irradiance of 130 suns. The improvement using the PhC absorber as compared to a blackbody absorber, both with the same PhC emitter, is about a factor of 2.3 at 130 suns, and overall the selective PhC absorber/emitter pair has a system efficiency that is 2.8 times higher than that of a blackbody absorber/emitter pair at 130 suns. The predicted maximum system

efficiency of the PhC absorber in this configuration is 5.5 % at 260 suns (normal incidence) reaching an operating temperature of 1500 K.

6. Experimental Section

Photonic crystal fabrication: The photonic crystal absorber and emitter were fabricated on the two sides of a double-side polished, 500 µm thick polycrystalline Ta 3%W alloy substrate (H.C. Starck) which was pre-annealed at 1755 K for 1.5 hours to ensure large grains and their thermal stability. The PhC pattern was defined by interference lithography (IL) and transferred into the Ta substrate by subsequent steps of reactive ion etching (RIE) using a Cr hard mask for the final deep RIE step of the Ta. For interference lithography, a tri-layer process was used and the final cavity diameter was defined by plasma ashing.[39] Reactive ion etching of the Cr hard mask using a SiO_2 mask ensures smooth cavity edges and good optical properties of the final PhC. The Ta is etched using an SF_6/C_4F_8 based Bosch process, achieving a final etch depth of up to 8 µm. Finally, the HfO_2 coating was deposited by ALD on the fabricated PhC, which ensures conformal coating in the high aspect ratio cavities, and good control over the final layer thickness. The thickness and refractive index of the HfO_2 layer was determined by spectroscopic ellipsometry using a Woollam VASE setup. The reflectance spectra of the fabricated absorbers were measured at room temperature using a Cary500 FTIR with an integrating sphere, capturing direct reflectance at near normal incidence (3°) as well as indirect reflectance from diffraction and scattering. No degradation of either the optical properties or the structure of the PhCs was observed after repeated STPV experiments at high temperature, as determined from repeated reflectance measurements and scanning electron micrographs before and after the high-temperature experiments.

STPV experiment:

In the experiments, the gap between the 2D PhC emitter and the PV cell was fixed at 300 µm, while a 1x1 cm square metal aperture was spaced 500 µm away from the absorber. The entire system was maintained in vacuum at pressures below 0.3 Pa to minimize conductive and

convective heat losses. The following experimental capabilities were used to measure the device characteristics: incident power of simulated solar radiation, current-voltage (I-V) characterization and temperature of the PV cell. The input power in our experiments was provided by a solar simulator (92192, Newport Oriel Inc.) with specific filters in place to match the AM1.5 direct spectrum. Light from the solar simulator was concentrated using a focusing lens system (Hi Flux Concentrator, Newport Oriel Inc.) and a secondary converging "light pipe" concentrator. The input power was determined shortly after each experiment by measuring the power through the aperture used in the experiment using a thermopile detector (919P-040-50, Newport Oriel Inc.). The output power was determined from the maximum power point of the I-V sweep taken using a precision source-meter (2440, Keithley Instruments Inc.) once the device reached steady state operation. A chilled water loop and cold plate (CP25, Lytron Inc.) were used to maintain the temperature of the PV cell near 293 K. Further details regarding the experimental layout can be found in the supplementary section of A. Lenert et al.[22]

Acknowledgements

The authors would like to thank James Daley and Tim Savas at NSL (MIT) for assistance in fabrication. Fabrication of Ta PhCs was done in part at the Nanostructures Laboratory (NSL) at MIT and at the Center for Nanoscale Systems (CNS) at Harvard University, a member of the National Nanotechnology Infrastructure Network (NNIN), which is supported by the National Science Foundation under NSF award No. ECS-0335765. We also thank H.C Starck for supply of the Ta 3% W substrates. This work was partially supported by the Army Research Office through the Institute for Soldier Nanotechnologies under Contract No. W911NF-13-D-0001. A. L., D. M. B., Y. X. Y., W. R. C., J. J. S., E. N. W. and M. S. were partially supported by the MIT S3TEC Energy Research Frontier Center of the Department of

Energy under Grant No. DE-SC0001299. V. R. gratefully acknowledges funding by the Austrian Science Fund (FWF): J3161-N20.

Received: ((will be filled in by the editorial staff))
Revised: ((will be filled in by the editorial staff))
Published online: ((will be filled in by the editorial staff))

[1] X. Wang, H. Li, X. Yu, X. Shi, J. Liu, *Appl. Phys. Lett.*, **2012,** *101*, 203109.

[2] Q.-C. Zhang, *J. Phys. D: Appl. Phys.*, **1999,** *32*, 1938.

[3] T. Sathiaraj, R. Thangarj, A. Sharbaty, M. Bhatnagar, O. Agnihotri, *Thin Solid Films,* **1990,** *190*, 241.

[4] C. E. Kennedy, *Review of mid- to high-temperature solar selective absorber materials*, Tech. Rep. TP-520-31267, National Renewable Energy, **2002**.

[5] S. Y. Lin, J. G. Fleming, D. L. Hetherington, B. K. Smith, R. Biswas, K. M. Ho, M. M. Sigalas, W. Zubrzycki, S. R. Kurtz, J. Bur, *Nature*, **1998**, *394*, 251.

[6] D. L. C. Chan, M. Soljačić, J. D. Joannopoulos, Phys. Rev. E **2006,** *74*, 036615.

[7] N. P. Sergeant, O. Pincon, M. Agrawal, P. Peumans, *Opt. Express* **2009**, *17*, 22800.

[8] P. Bermel, M. Ghebrebrhan, W. Chan, Y. X. Yeng, M. Araghchini, R. Hamam, C. H. Marton, K. F. Jensen, M. Soljačić, J. D. Joannopoulos, S. G. Johnson, I. Celanovic, *Opt. Express* **2010**, *18*, A314.

[9] E. Rephaeli, S. Fan, *Appl. Phys. Lett.* **2008,** *92*, 211107.

[10] N. P. Sergeant, M. Agrawal, P. Peumans, *Opt. Express* **2010,** *18*, 5525.

[11] C. Argyropoulos, K. Q. Le, N. Mattiucci, G. D'Aguanno, A. Alù, *Phys. Rev. B* **2013,** *87*, 205112.

[12] J. G. Fleming, S. Y. Lin, I. El-Kady, R. Biswas, and K. M. Ho, *Nature* **2002,** *417*, 52.

[13] X. Yu, Y.-J. Lee, R. Furstenberg, J. O. White, P. V. Braun, *Adv. Mater.* **2007**, *19*, 1689.

[14] C. Wu, B. Neuner, J. John, A. Milder, B. Zollars, S. Savoy, G. Shvets, *J. Opt.* **2012,** *14*, 024005.

[15] Y. Guo, C. L. Cortes, S. Molesky, Z. Jacob, *Appl. Phys. Lett.* **2012,** *101*, 131106.

[16] S. Molesky, C. J. Dewalt, Z. Jacob, *Opt. Express* **2013,** *21*, A96.

[17] V. Rinnerbauer, Y. X. Yeng, W. R. Chan, J. J. Senkevich, J. D. Joannopoulos, M. Soljačić, I. Celanovic. Opt. Express **2013**, *21*, 11482.

[18] K. A. Arpin, M. D. Losego, A. N. Cloud, H. Ning, J. Mallek, N. P. Sergeant, L. Zhu, Z. Yu, B. Kalanyan, G. N. Parsons, G. S. Girolami, J. R. Abelson, S. Fan, P. V. Braun, *Nat. Comm*. **2013,** *4*, 2630.

[19] K. A. Arpin, M. D. Losego, P. Braun, *Chem. Mater.* **2011,** *23*, 4783.

[20] P. Nagpal, D. P. Josephson, N. R. Denny, J. DeWilde, D. J. Norris, A. Stein, *J. Mater. Chem.* **2011,** *21*, 10836.

[21] A. Datas, C. Algora, *Prog. Photovolt: Res. Appl.* **2012**, *21*, 1099.

[22] A. Lenert, D. M. Bierman, Y. Nam, W. R. Chan, I. Celanovic, M. Soljačić, E. N. Wang, *Nat. Nano.* **2014**, *9*, 126.

[23] V. M. Andreev, A. S. Vlasov, V. P. Khvostikov, O. A. Khvostikova, P. Y. Gazaryan, S. V. Sorokina, N. A. Sadchikov, *J. Sol. Energy Eng.* **2007,** *129*, 298.

[24] N. P. Harder, P. Wurfel, *Semicond. Sci. Technol.* **2003,** *18*, S151.

[25] E. Rephaeli, S. Fan, *Opt. Express* **2009,** *17*, 15145.

[26] D. M. Trotter, Jr., A. J. Sievers, *Appl. Opt.*, **1980**, *19*, 711.

[27] A. F. Oskooi, D. Roundy, M. Ibanescu, P. Bermel, J. D. Joannopoulos, S. G. Johnson, *Comput. Phys. Commun.* **2010**, *181*, 687. http://ab-initio.mit.edu/meep (accessed Dec, 2013).

[28] V. Liu, S. Fan, *Comput. Phys. Commun.* **2012**, *183*, 2233. http://www.stanford.edu/group/fan/S4/ (accessed Feb, 2013)

[29] Y. S. Touloukian, D. P. DeWitt, *Thermophysical Properties of Matter, Vol. 7: Thermal Radiative Properties*, Plenum Press, New York, **1970**.

[30] S. G. Johnson, The NLopt nonlinear-optimization package, http://ab-initio.mit.edu/nlopt (accessed Dec, 2013).

[31] Y. X. Yeng, M. Ghebrebrhan, P. Bermel, W. R. Chan, J. D. Joannopoulos, M. Soljacic, I. Celanovic. *PNAS* **2012**, *109*, 2280.

[32] J. Wang, Z. Chen, D. Li, *phys. stat. sol. (a)*, **2010,** *207*, 1988.

[33] H. Sai, Y. Kanamori, H. Yugami, *Appl. Phys. Lett.* **2003,** *82*, 1686.

[34] C. Schlemmer, J. Aschaber, V. Boerner, J. Luther, *AIP Conf. Proc.* **2003,** *653*, 164.

[35] V. Stelmakh, V. Rinnerbauer, R. D. Geil, P. R. Aimone, J. J. Senkevich, J. D. Joannopoulos, M. Soljačić, I. Celanovic, *Appl. Phys. Lett.* **2013,** *103*, 123903.

[36] M. W. Dashiell, J. F. Beausang, H. Ehsani, G. Nichols, D. M. DePoy, L. R. Danielson, P. Talamo, K. D. Rahner, E. J. Brown, S. R. Burger, P. M. Fourspring, W. E. Topper, P. Baldasaro, C. A. Wang, R. K. Huang, M. K. Connors, G. W. Turner, Z. A. Shellenbarger, G. Taylor, J. Li, R. Martinelli, D. Donetski, S. Anikeev, G. L. Belenky, S. Luryi, *IEEE Trans. Electron Dev.* **2006,** *53*, 2879.

[37] Z.-P. Yang, L. Ci, J.A. Bur, S.-Y. Lin, P.M. Ajayan, *Nano Lett.* **2008**, *8*, 446-451.

[38] W. Chan, R. Huang, C. Wang, J. Kassakian, J. Joannopoulos, I. Celanovic, *Sol. Energy Mater. Sol. Cells* **2010**, *94*, 509–514

[39] V. Rinnerbauer, S. Ndao, Y. X. Yeng, R. D. Geil, J. J. Senkevich, K. F. Jensen, J. D. Joannopoulos, M. Soljačić, I. Celanovic, *J. Vac. Sci. Technol. B* **2013,** *31*, 011802.

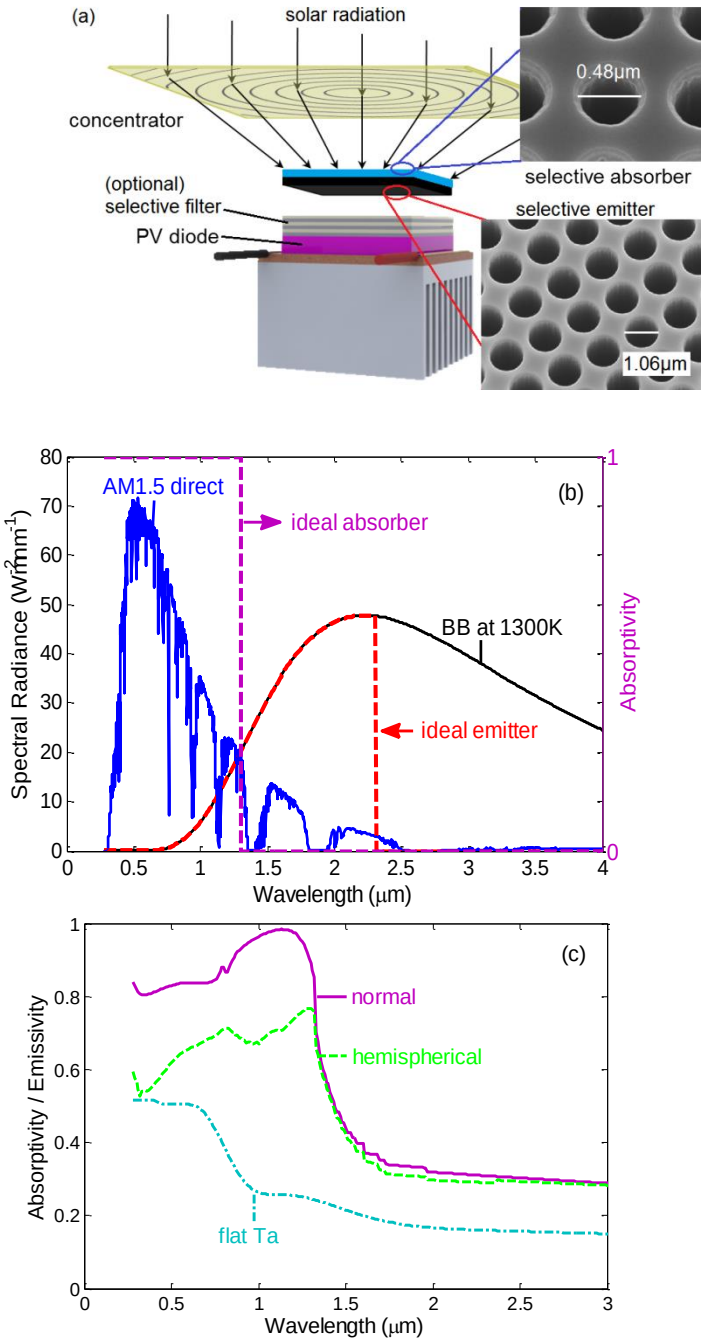

Figure 1. (a) Schematic concept of a solar TPV system with PhC absorber and emitter (inset: Scanning electron micrographs of the fabricated PhCs). (b) Incident solar spectrum (AM1.5D, 50 suns) and emission spectrum of a blackbody and an ideal emitter at 1300 K, as well as spectral absorptivity of ideal absorber. (c) Absorptivity of Ta PhC absorber optimized for 1000 K and 100 kWm^{-2} for normal incidence (solid line) and hemispherical emissivity (dashed) as well as normal absorptivity of a flat Ta substrate (dashed-dotted), using material dispersion of Ta at high temperature. For PhC parameters see Table 1.

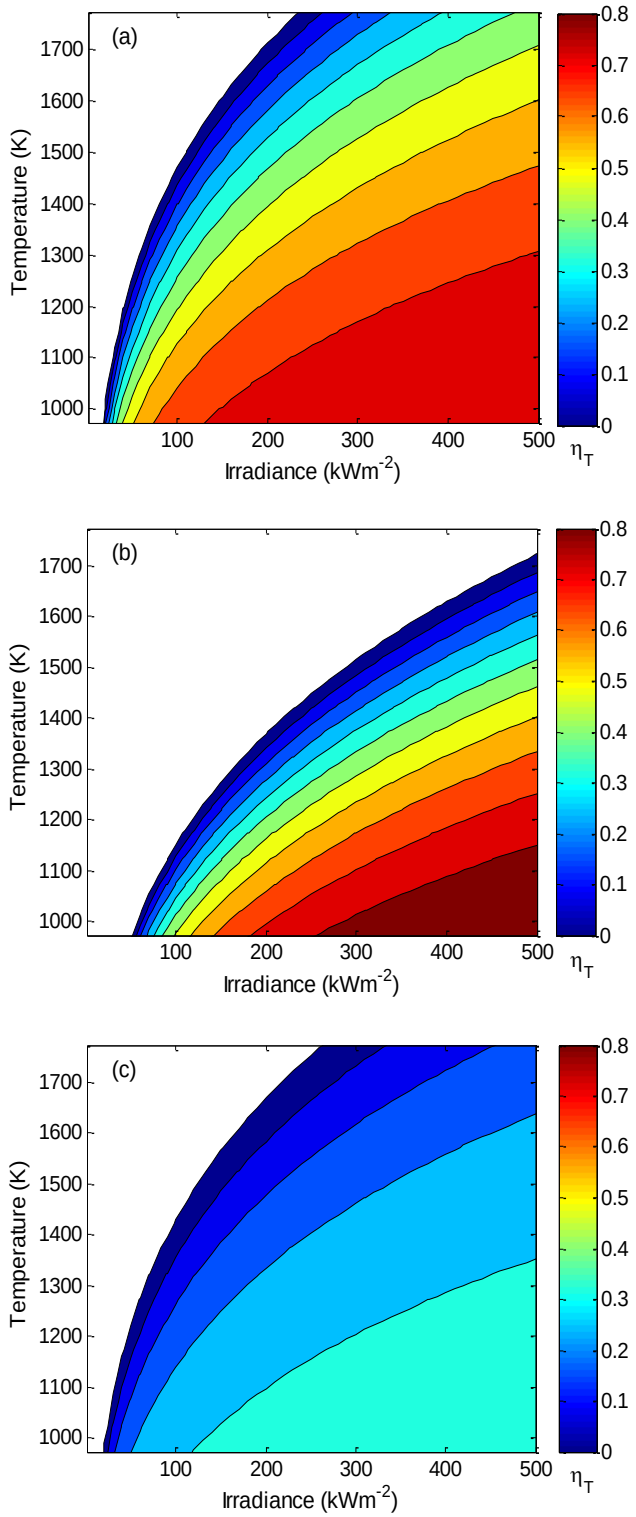

Figure 2. Calculated thermal transfer efficiency η_T comparing different absorbers: (a) Ta PhC, (b) blackbody, (c) flat Ta, as a function of incident irradiance at normal incidence and the absorber temperature.

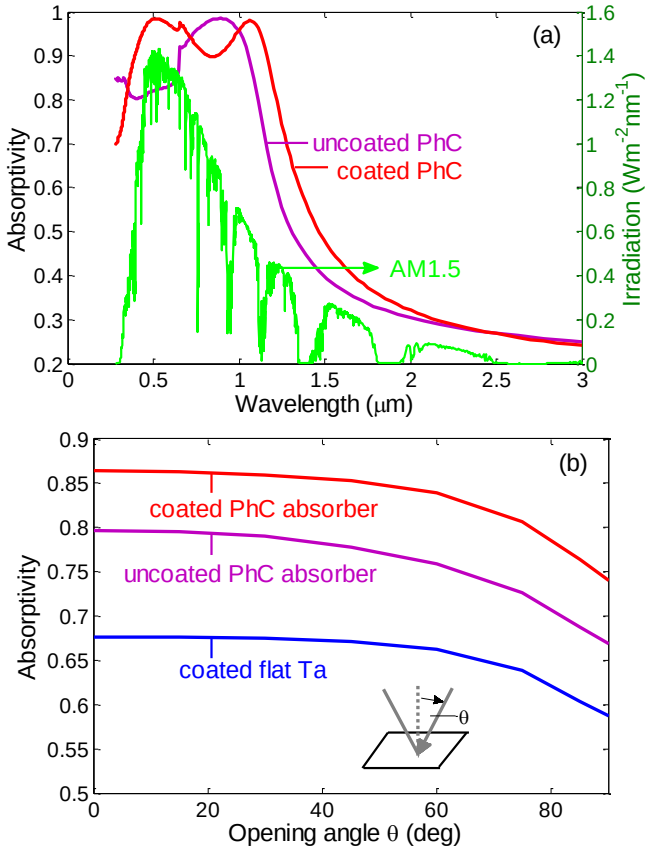

Figure 3. (a) Spectral absorptivity of coated and uncoated PhC absorber, optimized for 1300 K for normal incidence, and solar AM1.5D spectrum. (b) Dependence of solar absorptivity on the opening angle of incident radiation (see inset) for the optimized uncoated PhC absorber, the PhC absorber with optimized AR coating, and flat Ta with an AR coating of HfO_2. PhC parameters are listed in Table 1.

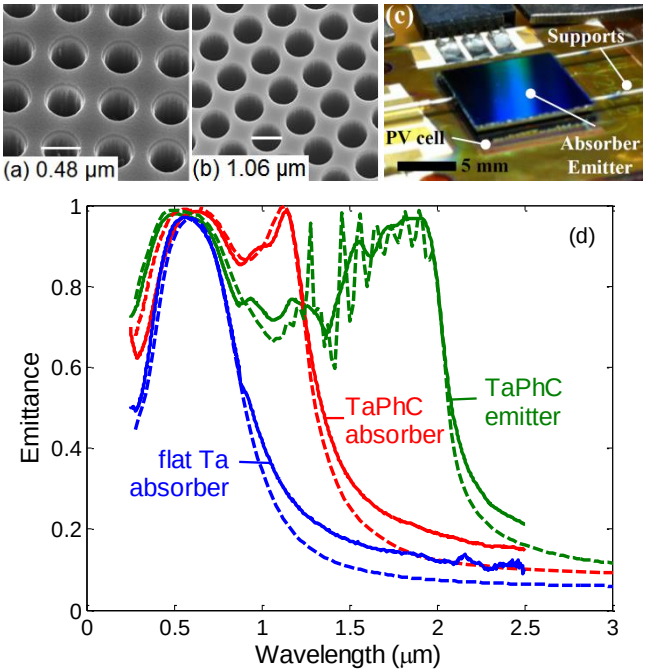

Figure 4. (a) Scanning electron micrograph of fabricated PhC absorber and (b) PhC emitter; (c) Photograph of absorber/emitter sample mounted on top of PV cell in STPV setup; (d) Normal emittance determined from reflectance measurements at room temperature (solid lines) and simulated normal emittance (dashed lines) of the fabricated PhC emitter, PhC absorber, and flat Ta absorber, all with HfO_2 coating. (PhC parameters see Table 1)

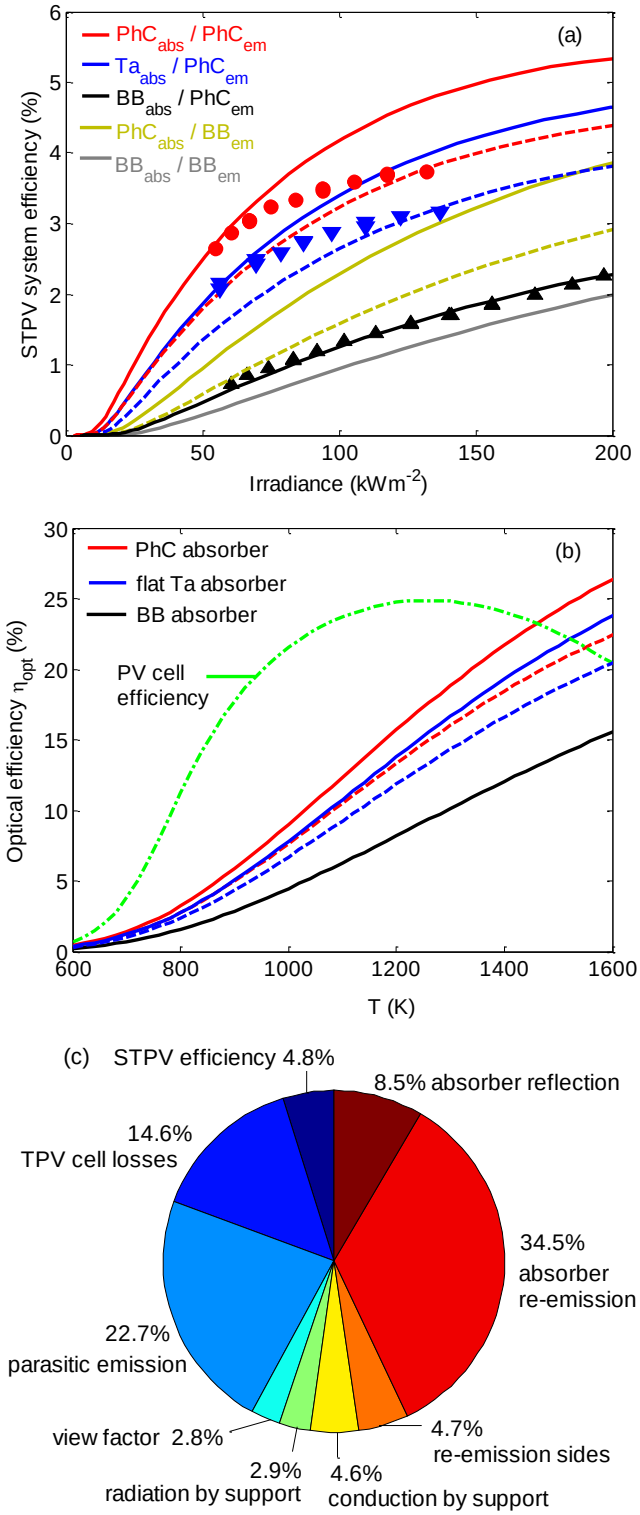

Figure 5. (a) Measured (symbols) and simulated (lines) system efficiency of an STPV system for different absorber/emitter pairs. The solid lines are modeled for irradiation at normal incidence, the dashed lines for the wide-angle incidence limit. (b) Total calculated optical conversion efficiency for different absorbers and PhC emitter for normal incidence, and PV cell efficiency (dashed-dotted). (c) Analysis of calculated losses as % of input power for the STPV system at 1300 K and normal incidence with the selective PhC absorber and emitter.

Table 1. Optimized parameters of the PhC absorbers and emitter for different operating conditions, and solar absorptivity $\bar{\alpha}$, thermal emissivity $\bar{\varepsilon}$ and thermal transfer efficiency η_T for the absorber and spectral efficiency η_{sp} for emitter, respectively, at these operating conditions.

absorber type	operating conditions	*r* [µm]	*a* [µm]	*d* [µm]	$\bar{\alpha}$	$\bar{\varepsilon}$	η_T
ideal cut-off absorber [a)]	1000 K 100 suns	-	-	-	0.956	0.039	0.931
blackbody	1000 K 100 suns	-	-	-	1	1	0.433
flat Ta	1000 K 100 suns	-	-	-	0.379	0.139	0.300
2D PhC	1000 K 100 suns	0.34	0.78	8.0	0.810	0.256	0.664
2D PhC uncoated	1300 K STPV	0.28	0.66	4.6	0.797	0.269	0.471
2D PhC coated (40 nm HfO_2)	1300 K STPV	0.24	0.66	4.6	0.864	0.262	0.517
PhC emitter, coated (35 nm HfO_2)	1300 K	0.53	1.28	7.0	-	0.358	0.471 [b)]

a) $\lambda_{cut\text{-}off} = 1.8$ µm

b) for the emitter: η_{sp} for $\lambda_{PV} = 2.3$ µm at 1300 K, as defined in Equation 7

Table of Contents:

A tunable and highly spectral selective absorber/emitter based on 2D PhCs fabricated on a single flat Ta substrate is demonstrated for high-temperature solar thermal energy conversion, and optimized for a solar thermophotovoltaic application. The measured system efficiency shows significant improvement using the PhC absorber relative to a blackbody absorber in the same configuration, as predicted by a detailed system model.

Keyword Photonic Crystals

V. Rinnerbauer,* A. Lenert, D. Bierman, Y. X. Yeng, W. R. Chan, R. D. Geil, J. J. Senkevich, J. D. Joannopoulos, E. N. Wang, M. Soljačić, I. Celanovic

Metallic Photonic Crystal Absorber-Emitter for Efficient Spectral Control in High-Temperature Solar Thermophotovoltaics

ToC figure